

Article

Structural, Mechanical and Chemical Properties of Low Content Carbon Geopolymer

Snežana Nenadović¹, Jelena Gulicovski^{1,*}, Miljana Mirković¹, Ljiljana Kljajević¹, Ivana Bošković², Mira Vukčević² and Miloš Nenadović³

¹ Department of Materials Science, “VINČA” Institute of Nuclear Science, National Institute of the Republic of Serbia, University of Belgrade, 11000 Belgrade, Serbia; msneza@vinca.rs (S.N.); miljanam@vinca.rs (M.M.); ljiljana@vinca.rs (L.K.)

² Faculty of Metallurgy and Technology, University of Montenegro, Cetinjski Put bb, 81000 Podgorica, Montenegro; ivabo@ucg.ac.me (I.B.); mirav@ucg.ac.me (M.V.)

³ Department of Atomic Physics, “VINČA” Institute of Nuclear Science, National Institute of the Republic of Serbia, University of Belgrade, 11000 Belgrade, Serbia; milosn@vinca.rs

* Correspondence: rocenj@vin.bg.ac.rs

Abstract: In recent years geopolymers have shown increased interest as binders with low CO₂ emission compared to Portland cement. The main goal of this research is focused on connecting green and sustainable characteristics with the mechanical and chemical properties of fly ash-based geopolymer. The samples of different ratios of fly ash (FA) and metakaolin (MK) were prepared. X-ray powder diffraction (XRD) showed that in the geopolymer synthesis reaction a new amorphous phase was formed. Diffuse reflectance infrared Fourier transform spectroscopy (DRIFT) confirmed characteristic bands of the Si-O and O-Si-O groups at 1045 cm⁻¹. Compressive strength analysis revealed that the optimal ratio of FA and MK is 50:50 and exhibits the highest value. X-ray photoelectron spectroscopy (XPS) analysis revealed the total reduction of carbon content in the alkali-activated geopolymer with the optimal stoichiometry of 50:50. This indicates the possibility of obtaining a geopolymer material with an almost complete absence of carbon, which implies further application as a material with a very high environmental potential and of zero carbon emissions.

Keywords: carbon reduction; compressive strength; geopolymer; metakaolin; fly ash; XPS



Citation: Nenadović, S.; Gulicovski, J.; Mirković, M.; Kljajević, L.; Bošković, I.; Vukčević, M.; Nenadović, M. Structural, Mechanical and Chemical Properties of Low Content Carbon Geopolymer. *Sustainability* **2022**, *14*, 4885. <https://doi.org/10.3390/su14094885>

Academic Editor: Mariateresa Lettieri

Received: 18 March 2022

Accepted: 11 April 2022

Published: 19 April 2022

Publisher's Note: MDPI stays neutral with regard to jurisdictional claims in published maps and institutional affiliations.



Copyright: © 2022 by the authors. Licensee MDPI, Basel, Switzerland. This article is an open access article distributed under the terms and conditions of the Creative Commons Attribution (CC BY) license (<https://creativecommons.org/licenses/by/4.0/>).

1. Introduction

Green material engineering is very important because it encourages sustainable development and reduces the emission of pollutants into the atmosphere. Metakaolin as well as industrial mineral kaolin and fly ash from the thermal power plant process are recognized as such. The manufacture of building materials such as Portland cement has a negative impact on the environment. In recent years this fact has provided a huge impetus for the increased use of waste and by-products in the production of concrete instead of Portland cement. Activating aluminosilicate materials such as fly ash and blast furnace slag using alkaline solutions to produce new binders is a major advance towards increasing the usefulness of industrial waste products [1–3] and reducing the adverse impacts during cement production. These bonding systems can be found in the scientific literature under various names: alkali-activated cement, geopolymers [4–7], inorganic polymers [8], and low-temperature aluminosilicate glass. They are also called polysilanes because of the silicon-oxygen-aluminum polymer frame [9]. Geopolymers are usually obtained from natural, raw aluminosilicate materials and materials such as industrial and natural wastes [10]. These materials have been attracting a lot of attention lately because the carbon footprint is far smaller than with cement binders. The reduction in total CO₂ emissions in the synthesis of geopolymers is achieved by choosing the right activator and the appropriate stoichiometry of the desired material [5]. Through geopolymerization/the alkali-activation process traces of toxic metal elements can be caught from fly ash or external sources [11].

The type and concentration of the starting material and activating solutions are the most important parameters that affect the properties of the final product [6]. Previous studies have shown that the amount of vitreous silicon and alumina present in the starting material plays a significant role in the activation reactions and the properties of the reaction product [12,13]. Environment-friendly civil engineering as a challenging issue has become crucial for the development of economical and relatively low-cost building materials. It was previously determined that concretes containing alkali-aluminosilicate gel as a binder have high compressive strength and resistance to fire and chemical attack, bearing in mind that geopolymer can be an adequate replacement for cement. In addition, cement consumes a lot of energy and emits gasses into the environment in its production [14]. Compared to MK geopolymer, studies on pure fly ash alkaline-activated materials have shown that fly ash geopolymer has low reactivity. Heat treatment is also usually necessary to achieve good structural and mechanical properties. Observing the development and application of technologies related to the application of fly ash, it was moved from the category “Waste material” to the category “Resource material”. There is a useful potential for fly ash in the field of civil engineering construction, as well as others [15]. Antonella Petrillo et al. [16] have reported that geopolymers have emerged as novel engineering materials with the potential to form a substantial element in an environmentally sustainable construction and building products industry. Geopolymeric blocks are considered as a new family of eco-sustainable masonry units because they widen the possibilities to recycle waste into useful products, especially building materials that can contribute environmental and economic benefits. The first mechanisms of the synthesis of these materials have been explored; in addition, our contributions, as well as the research of our colleagues, means we have established international cooperation in this area and in the other mechanisms of synthesized materials related to the various elements of environmental protection (carbonation, alkali silica, acid resistance, high temperature resistance, freezing, etc.). Our proposal deals with all these important parameters in a systematic manner, and always keeps in mind how to adjust the parameters of material technological aspects. Namely, it is estimated that infrastructure rehabilitation costs go into the trillions of dollars; for the 84,000 concrete bridges in the European Union alone, the annual cost for maintenance and repair is 215 million £ [17], while in the U.S.A. the annual cost of repair, protection, and strengthening is estimated to be between 15 and 22 billion \$ [18]. This is a sufficient reason to research and synthesize new materials that are good alternatives to Portland cement, both economically and primarily in terms of environmental protection. In this sense, geopolymers are increasingly being used in the construction sector. Considering that, the aim of this research was to investigate the effect of the composition of fly ash and metakaolin on the compressive strength of the obtained geopolymer samples with low CO₂-emission, that would find application as low cost and eco-friendly construction materials in the building industry.

2. Materials and Methods

2.1. Raw Materials

The fly ash (FA) and metakaolin (MK) as precursors were used in this study. The clay originated from Rudovci (Serbia) [19], while the FA originated from a coal fired power station—Pljevlja, Montenegro. Metakaolin was prepared by thermal treatment clay at 750 °C in an air atmosphere with a heating rate of 10° /min and soaking time at an elevated temperature of one hour. The clay was dried, ground and then sifted through a sieve. Activation solution was prepared using the appropriate amounts of sodium hydroxide (NaOH-analytical grade) dissolved in high purity water (18.2 MΩ). The Na₂SiO₃ solution was added (technical grade, supplied by a manufacturer from Serbia, “DEM Company”, Belgrade, the chemical composition of Na₂SiO₃ was comprised of Na₂O = 14.7%, SiO₂ = 29.4%, and water 55.9%). The alkali activator of 12 M NaOH and solution of Na₂SiO₃ was prepared by a magnetic stirrer. The ratio of these two solutions was 1.5. The solutions were stirred for 2 h before use.

2.2. Geopolymer Synthesis

Geopolymer samples were synthesized by alkaline-activation of a series of blends of FA and MK. The liquid/solid (L/S) mass ratios were kept in the range of 0.8–1.0, depending on the acceptable workability of each sample. The actual water to solid (binder) (w/b) ratios are 0.40–0.50 for samples. The waste fly ash powder and MK as solid components and the alkali silicate activator were mixed until a homogenous slurry was formed. The prepared pastes were cast in cylindrical molds (diameter-12 mm/height-26 mm) and compacted on a vibrating table.

Table 1 presents the mix designs for all geopolymer samples. Four starting mixtures were prepared by homogenization of the thermally treated clay (Metakaolin) and fly ash in the amounts which are presented in Table 1.

Table 1. Details of mixtures composition.

Samples	Fly Ash, (FA) %	Metakaolin (MK), %
GP ₁₀₀₋₀	100	0
GP ₇₀₋₃₀	70	30
GP ₅₀₋₅₀	50	50
GP ₃₀₋₇₀	30	70

Based on previous research and determining optimal conditions for curing and aging, the samples were packed in a plastic bag to prevent drying, cured at 80 °C for 2 days in a drying oven and then were transferred to the box at room temperature and relative humidity of 95%, until mechanical testing was conducted [6–8]. The prepared samples were denoted by GP_{x-y}, by the processing conditions: x-content of fly ash; y-content of metakaolin.

2.3. Characterization Techniques

Chemical compositions of the starting and geopolymer materials, obtained by the X-ray fluorescence XRF analysis (Rigaku NEX ED-High Resolutions ED-XRF Elemental Analyzed), are shown below.

Table 2 shows the chemical composition of fly ash and metakaolin samples, while Table 3 shows the SiO₂/Al₂O₃ and Na₂O/Al₂O₃ ratio of synthesized geopolymer materials.

Table 2. Chemical composition of fly ash and metakaolin.

Samples	SiO ₂	Al ₂ O ₃	Fe ₂ O ₃	CaO	Na ₂ O	MgO	P ₂ O ₅	TiO ₂	K ₂ O	MnO	LOI
Fly ash	48.95	22.65	4.23	12.94	1.50	3.42	0.63	0.70	2.80	0.07	2.11
Metakaolin	51.70	31.89	5.23	2.05	1.35	5.45	/	/	0.95	/	1.38

Table 3. The SiO₂/Al₂O₃, Na₂O/Al₂O₃ ratio of the geopolymer materials.

Samples	SiO ₂ /Al ₂ O ₃	Na ₂ O/Al ₂ O ₃
GP ₁₀₀₋₀	2.25	0.49
GP ₇₀₋₃₀	2.18	0.50
GP ₅₀₋₅₀	1.97	0.45
GP ₃₀₋₇₀	1.80	0.55

Mineralogical characterization of the geopolymer samples was conducted using X-ray powder diffraction (XRD) Ultima IV Rigaku diffractometer, with Cu K α _{1,2} line, the output voltage of 40.0 kV and a working current of 40.0 mA. Spectrum 2 θ range was from 5° up to 80°. This setting was used for all powders, the scanning step was maintained at 0.02° at a rate of 5°/min. For phase analysis of samples, PDXL2 software (Ver. 2.8.4.0, Rigaku, Tokyo, Japan) was used equipped with an ICDD database: quartz (01-089-8936), pyrophyllite (01-073-4051), wollastonite (01-083-2198), kaolinite (01-075-0938), illite (00-043-0685), hematite (01-076-4579), and lime (01-082-1691).

Diffuse reflectance infrared Fourier transform spectroscopy (DRIFTS) is a cheap, fast and non-destructive way of evaluating clay minerals and their products (Ray and Johansson, 1998). Drift spectra were obtained using the PerkinElmer FTIR spectrometer Spectrum Two. (Waltham, MA, USA). Approximately 5% of samples were dispersed in oven-dried spectroscopic grade KBr with a refractive index of 1.559 and particle size of 5–20 μm . The spectra were scanned at 4 cm^{-1} resolution and collected in the mid-IR region from 4000 to 400 cm^{-1} .

X-ray photoelectron spectroscopy (XPS) analysis was performed using a SPECS instrument (Berlin, Germany) for detailed chemical composition characterization, using X-ray-induced photoelectron spectroscopy. Photoelectron emission was excited by the monochromatic Al $K\alpha$ line with a photon energy of 1486.67 eV. Detailed spectra of the main photoelectron lines were taken in the fixed analyzer transmission mode with a pass energy of 20 eV (FAT 20), an energy step of 0.1 eV, and a dwell time of 2 s. Charging compensation was performed using an electron flood gun and the constant current and voltage. The binding energy axis was adjusted according to the position of the carbon C 1 s line. The survey spectra were performed according to the characteristic spectral line intensities. Specific atomic sensitivity factors for each analyzed element were used to eliminate the background lines, provided by the manufacturer.

The field emission scanning electron microscopy (FESEM) and instrument TESCAN Mira3 XMU at 20 kV (Tescan, Brno-Kohoutovice, Czech Republic) were used for the investigation of the morphological and microstructural properties of obtained geopolymer samples. Before analysis, the samples were pre-coated with several nanometers thick gold layer, using the sputter coater Polaron SC503 Fision Instrument (Quorum Technologies Ltd., Lewes, UK).

Bulk densities (ρ) were measured by the Archimedes method. The compressive strength of the given samples was performed on an HPN400 type press (ZRMK-Ljubljana). The compression tests were performed after 28 days aging at room temperature. One can observe that, at this stage, oven-cured geopolymers have almost gained the maximum compressive strength.

3. Results and Discussion

Geopolymerization is a complex multiphase process that includes a series of dissolution, reorientation, and solidification reactions. Hence, the dissolution of Si and Al species from solid sources under alkaline conditions plays a significant role in the reactivity of raw material for geopolymerization (Ivanović et al., 2020).

3.1. X-ray Diffraction (XRD)

The XRD results of starting powders: FA and MK are shown in Figure 1.

The mineralogical composition of MK consists predominantly of the clay minerals illite, and kaolinite, with quartz as a secondary mineral. The mineralogical composition of FA indicates peaks that belong to clay minerals and quartz. In addition, there are peaks belonging to lime (calcium oxide), as well as minerals such as wollastonite (calcium silicon oxide) and pyrophyllite (aluminum silicate). Based on the presented results, mineral composition is in accordance with the chemical composition of FA because the calcium content in fly ash is significantly higher than in metakaolin.

The geopolymer is formed by the alkaline activation of the solid phase (metakaolin and fly ash) with an alkaline activator. The characteristic background halo that appears in the geopolymer samples in the range from 15° to $40^\circ 2\theta$ is very intensively expressed. As the proportion of fly ash increases, so does this halo. The surface area of this halo is an indicator of the amorphousness of the sample, which means that, as the proportion of fly ash increases, the proportion of the amorphous phase that participates in the geopolymer synthesis reaction and contributes to the creation of a new amorphous phase of geopolymer samples increases. Quartz is the major phase in all four samples, followed by the appearance of pyrophyllite and wollastonite [20]. Based on the results, geopolymer samples are

amorphous to semicrystalline aluminosilicates [21]. Crystalline phases which are identified in raw materials, especially clay minerals, disappear in geopolymer specimens. MK with high amorphous phases content is the dominant component of geopolymer production, while crystalline phases such as quartz, wollastonite, and pyrophyllite still exist in geopolymer samples in a semicrystalline form. According to literature data, the presence of wollastonite in geopolymer samples could contribute to particle reinforcement [22].

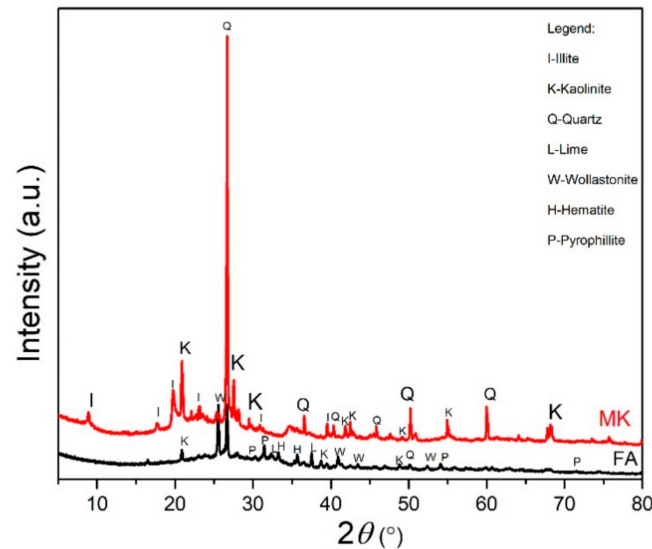


Figure 1. XRD patterns of FA and MK.

The XRD patterns of the geopolymer samples: GP₁₀₀₋₀, GP₇₀₋₃₀, GP₅₀₋₅₀, and GP₃₀₋₇₀ are shown in Figure 2.

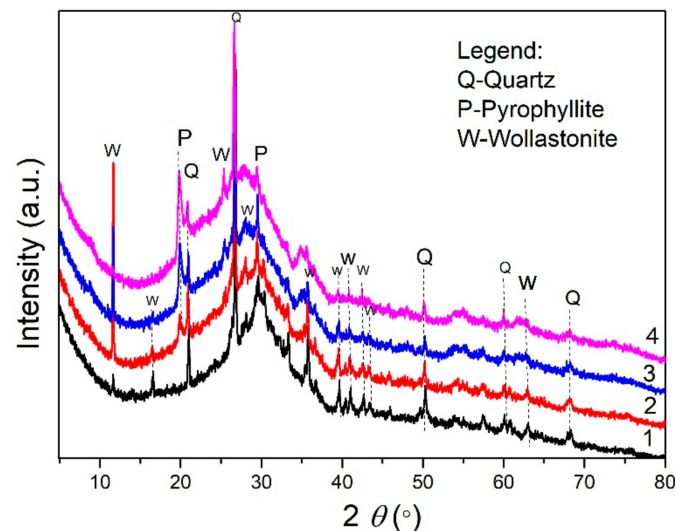


Figure 2. XRD patterns of the samples: (1) GP₁₀₀₋₀; (2) GP₇₀₋₃₀; (3) GP₅₀₋₅₀; and (4) GP₃₀₋₇₀.

3.2. DRIFT Analysis

The DRIFT spectra of geopolymer samples are shown in Figure 3. This figure shows that the wide band that occurred around 3500 cm^{-1} is due to the stretching vibrations of O-H bonds and H-O-H bending vibrations of the interlayer-adsorbed H_2O molecule [20]. The peak at 1620 cm^{-1} corresponds to the H-O-H bending vibration too. The absorption bands at 2813 cm^{-1} were related to symmetric aliphatic $-\text{CH}_2$ groups [23]. A peak observed in the DRIFT spectra around 1450 cm^{-1} was assigned to stretching vibrations of O-C-O bonds, possibly indicating atmospheric carbonation [24].

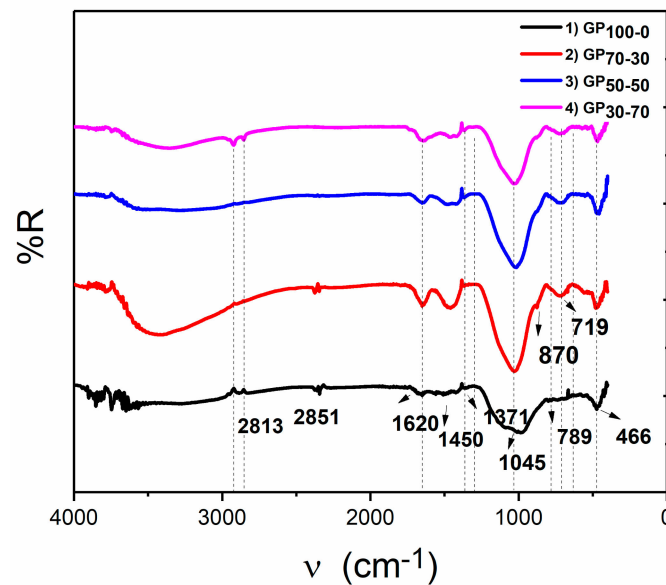


Figure 3. DRIFT spectra of the geopolymer samples (1) GP₁₀₀₋₀; (2) GP₇₀₋₃₀; (3) GP₅₀₋₅₀; and (4) GP₃₀₋₇₀.

The main reason is the presence of chemisorbed CO₂ in MK/FA geopolymer samples or which might be formed from the remaining unreacted activator solution and CO₂ [25–27]. The band at approximately 1100 cm⁻¹ is assigned to the Si-O stretching in tetrahedrons [4,28,29]. Characteristic bands of the Si-O and O-Si-O groups are observed at 1045 cm⁻¹ confirming the presence of silicate groups. As a result of the alkaline activation process of the MK/FA precursors, the geopolymer samples were obtained. The Si-O-Al asymmetric stretch band overlaps with peaks that correspond to the Si-O or Si-O-Si stretching vibrations. The peaks at 1100–440 cm⁻¹ in relation to Si-O-Si, Al-O-Si are asymmetric and symmetric stretching and bending vibrations. The peaks at 789 cm⁻¹ and 466 cm⁻¹ correspond to the symmetric Si-O stretching vibrations of quartz [30].

3.3. XPS Analysis

XPS analysis was performed for samples GP₁₀₀₋₀ and GP₅₀₋₅₀. The reason why these two samples were chosen is that they show the greatest difference in composition and in terms of total carbon reduction, revealed by DRIFT.

The survey spectrum of sample GP₁₀₀₋₀ is shown in Figure 4a. It is the starting material made up of pure fly ash. As can be expected, it contains various elements that are present in the ash as a result of the combustion process. O1s and C1s peaks are the most dominant. The C1s peak is at the expected binding energy value of 285.0 eV, and represents 47.15 atomic percentages of the sample. The splitting of the carbon peak originates from the presence of organic and adsorbed carbon. Organic carbon is at higher binding energy values, while the adsorbed and carbide carbon is at lower bond energy values. The presence of different carbon contributions is a consequence of the heterogeneity of the starting material due to its natural origin. Analysis of the O1s peaks of the GP₁₀₀₋₀ sample as the starting material (Figure 4b) shows the splitting of the peaks into three dominant contributions. The situation is quite complex due to the existence of a lot of oxygen compounds that can be formed during the combustion process. At lower values of the binding energy (530.3 eV), there is a contribution derived from metal oxides (O1s/1). The higher values are the oxygen that comes from adsorption (O1s/2) at 532.4 eV as well as the bound organic oxygen at about 534.2 eV (O1s/3). In the initial sample, GP₁₀₀₋₀ aluminum is quite underrepresented. The Al 2s line at about 115 eV and the Al 2p line at about 77eV make up a total of about eight atomic percentages of the total sample. By detailed analysis of the XPS spectra of aluminum (Figure 4c.), the more dominant contribution of the Al 2p spectral line has been fitted. The analysis shows unequivocally that the distribution of aluminum in the initial

sample is very homogeneous and originates from only one type of aluminum oxide, Al_2O_3 , at 76.8 eV.

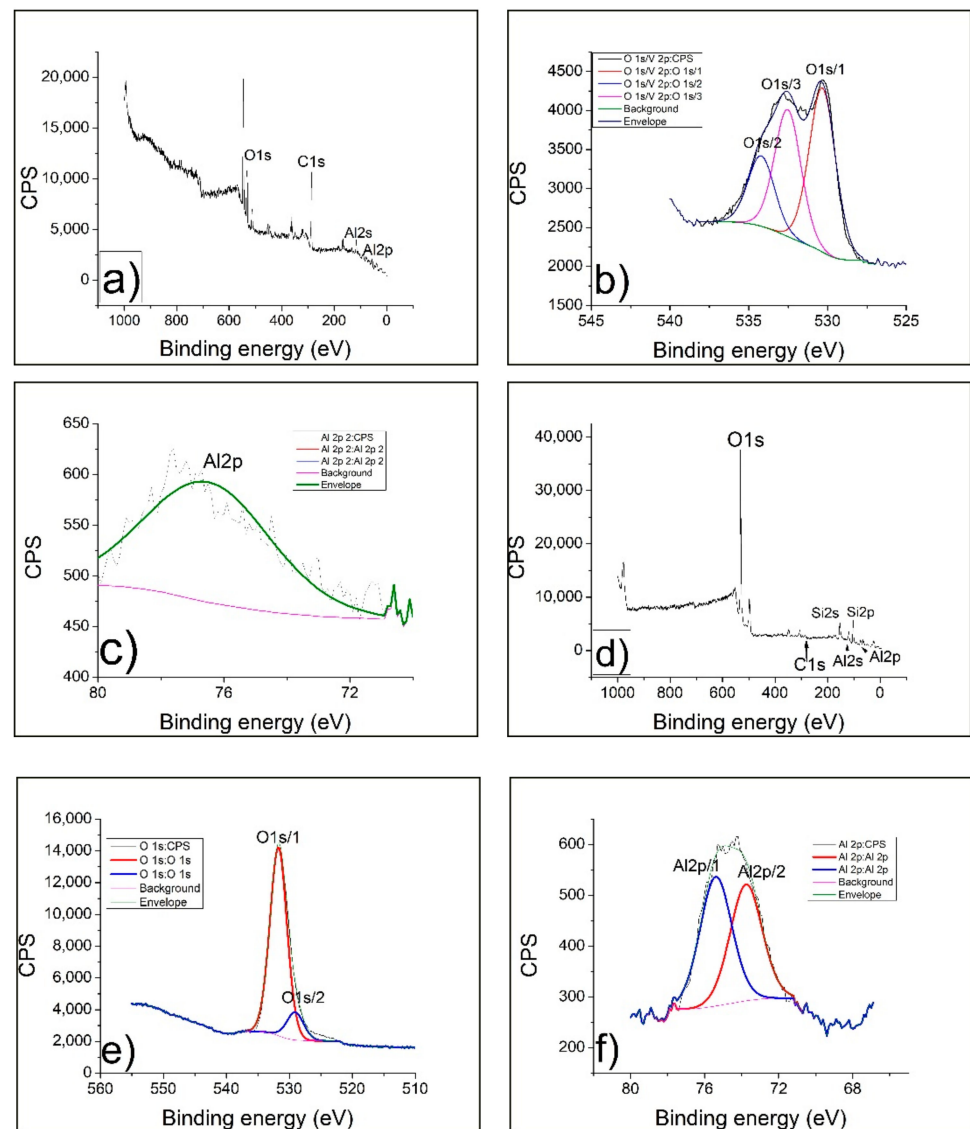


Figure 4. (a) Survey spectrum of GP100-0; (b) Detailed spectra O1s of GP100-0; (c) Detailed spectra Al 2p of GP100-0; (d) Survey spectrum of GP50-50; (e) Detailed spectra O 1s of GP50-50; (f) Detailed spectra Al 2p of GP50-50.

After the process of alkaline activation, using NaOH and Na_2SiO_3 , in the sample G_{50-50} , there were significant changes in the chemical composition. Figure 4d shows a drastic jump in the oxygen line at the position of 533.7 eV. This was expected, bearing in mind that the starting sample was treated with oxygen chemicals. It represents the dominant spectral line, while the carbon concentration dropped to almost zero. This stoichiometric ratio of the constituents of the GP_{50-50} geopolymer shows the best degree of carbon reduction. It is extremely important that the concentration of carbon that was about 47.15 at % fell almost to zero and it is impossible to analyze it further. A very small peak C 1s in Figure 4d (marked with an arrow) is located at 283.7 eV. By detailed analysis of the O1s spectral line (Figure 4e), it can be concluded that the existing oxygen can be defined by two contributions. Alkaline treatment reduces the number of contributions and chemical bonds that oxygen forms in the geopolymer. The dominant contribution of the O 1s/1 spectral line is at 531.7 eV. It points out that there was an alkaline activation of the initial sample and

the given spectral line refers to Si-O-Si bonds. The second, smaller contribution of oxygen at 529.1 eV may come from unreacted Al and Si units. In this way, the oxides present in the starting sample remained in small quantities and in the geopolymer material. The detailed spectrum of the Al 2p spectral line (Figure 4f) reveals two almost equal contributions of Al in the geopolymer. The first line Al 2p/1, located at 75.4 eV, speaks about the degree of reaction of the starting material with alkaline precursors. It refers to the Al-O-Si bond formed from Al_2O_3 and $\text{Al}(\text{OH})_3$. Another contribution of almost equal intensity Al 2p/2 speaks of a lower degree of geopolymerization reaction and the presence of a larger amount of unreacted Al_2O_3 with silicate precursors. This peak is located at a lower bond energy value of 73.7 eV. Observing the overall effect of the geopolymerization process in the case of sample G_{50-50} , it can be concluded that the total reaction rate, in this case, is about 50%, but the carbon reduction is almost complete.

3.4. Morphological and Microstructural Analysis

The FESEM analysis was performed for all four geopolymer samples shown in Figure 5. The preliminary images of the samples GP_{100-0} and GP_{70-30} at a magnification of 1.0 KX (Figure 5a,b) show an even distribution of pores and a much smaller number of microcracks compared to Portland cement mortars [31]. The relatively uniform distribution of pores and cracks indicates homogeneity in the structure of the starting constituents and reactants. Stoichiometry in these two cases leads to the formation of smaller spheres and microcracks. Samples of GP_{50-50} and GP_{30-70} on the same magnification of 1.0 KX show much larger phenomena on the surface in the form of larger spheres and holes (Figure 5c,d). This is definitely a consequence of the change in the ratio of MK and FA, where, with the increase in the amount of FA, a swelling reaction occurs and the particles of fly ash crack. In addition, the process of coalescence and merging into larger spheres is noticeable. This microstructure has a favorable effect on increasing the compressive strength, especially in the case of the GP_{50-50} sample which shows the maximum.

Otherwise, SEM analysis of the same geopolymer samples was completed on the magnification of 10.0 KX and 21.0 KX. (Figure 6). A more detailed insight into the microstructure of the obtained geopolymers can be extracted from the given figures. In Figure 6, white arrows mark areas richer in fly ash, while yellow arrows mark areas richer in metakaolin. As can be seen in all the pictures, the most pronounced is the morphology which indicates the degree of hydration. In addition, fractions of unreacted components are observed in the geopolymer matrix. According to XPS analysis, the average degree of reaction process is about 50%.

In Figure 6a one can notice the existence of unreacted fly ash as well as hydration products on sample GP_{100-0} . The geopolymer matrix is very homogeneous due to its stoichiometric composition since it consists of pure fly ash. Figure 6b shows the sample GP_{70-30} on which spheres of partially unreacted fly ash with a diameter of about 3 microns can be seen. By the magnification of 21.0 KX, on the surface of the spheres are visible hydration products, as a consequence of the geopolymerization reaction. Incorporated into the geopolymer matrix is also the partially reacted metakaolin. SEM analysis of the sample with the optimal stoichiometry of metakaolin and fly ash in a ratio of 50:50 (Figure 6c) shows slightly smaller spheres of unreacted fly ash and a more homogeneous distribution of the also unreacted metakaolin.

In Figure 6a, one can notice the existence of unreacted fly ash, as well as hydration products on sample GP_{100-0} . Geopolymer matrix is very homogeneous due to its stoichiometric composition since it consists of pure fly ash. Figure 6b shows sample GP_{70-30} , on which spheres of partially unreacted fly ash with a diameter of about 3 microns can be seen. By the magnification of 21.0 KX, on the surface of the spheres are visible hydration products, as a consequence of geopolymerization reaction. Incorporated into the geopolymer matrix is also partially reacted metakaolin. SEM analysis of the sample with the optimal stoichiometry of metakaolin and fly ash in a ratio of 50:50 (Figure 6c) shows slightly smaller spheres of unreacted fly ash and a more homogeneous distribution of also unreacted metakaolin.

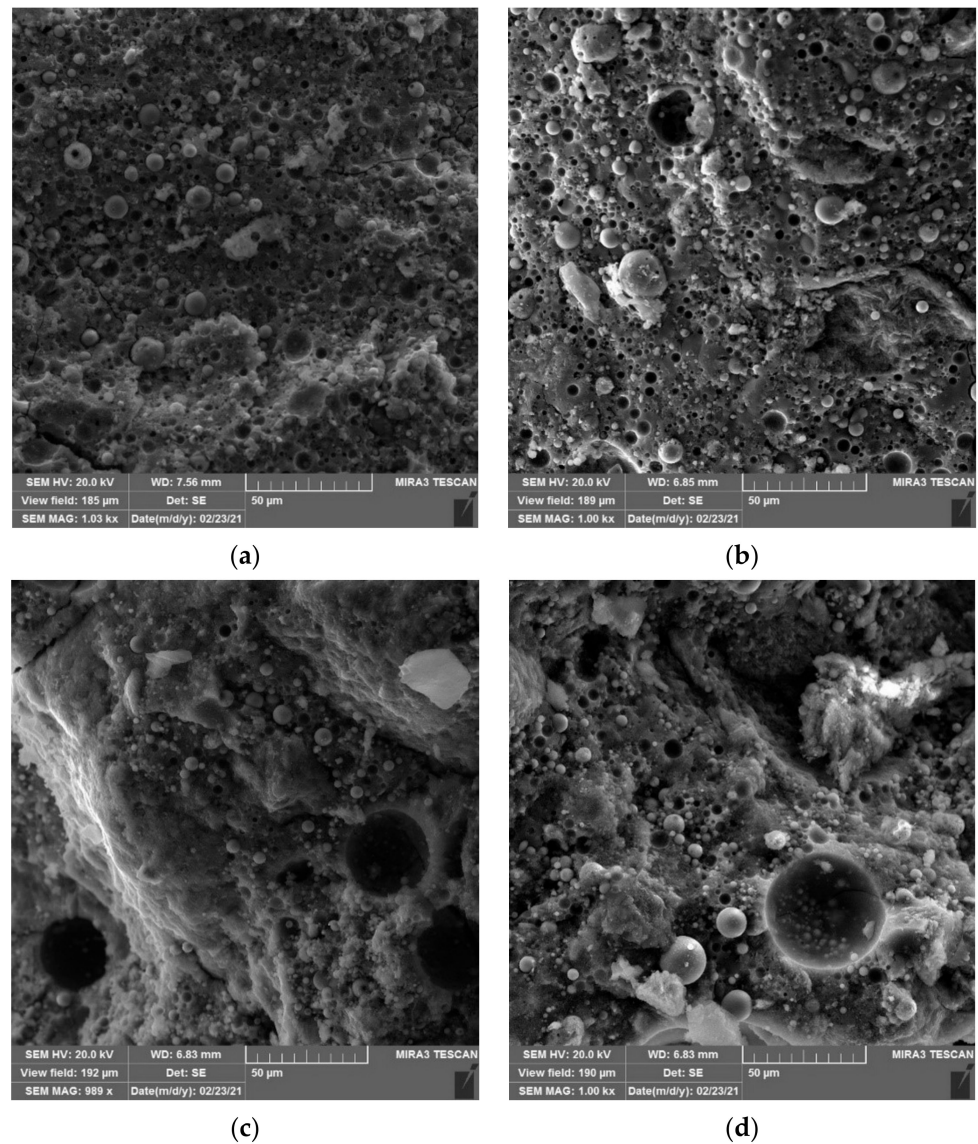


Figure 5. FESEM image of the geopolymer samples (a) GP₁₀₀₋₀; (b) GP₇₀₋₃₀; (c) GP₅₀₋₅₀; and (d) GP₃₀₋₇₀.

It should be emphasized that the sample GP₅₀₋₅₀ (Figure 6c) based on XPS analysis showed a complete absence of carbon. This is an important fact, because it affects both the chemical and mechanical properties of the geopolymer. The absence of carbon in the geopolymer matrix led to the formation of a more tightly bound structure within the Si-O-Si groups. This resulted in increased compressive strength and lower specific density. The obtained material is strong enough, but also light compared to other geopolymer samples. Figure 6d represents a sample having an excess of metakaolin in its composition GP₃₀₋₇₀ (70%). It can be noticed that the unreacted metakaolin is in excess and spreads over almost the entire surface of the sample. Spheres of unreacted fly ash are present but to a lesser extent consistent with stoichiometry. As with all other geopolymer samples, hydration products are present, without exception.

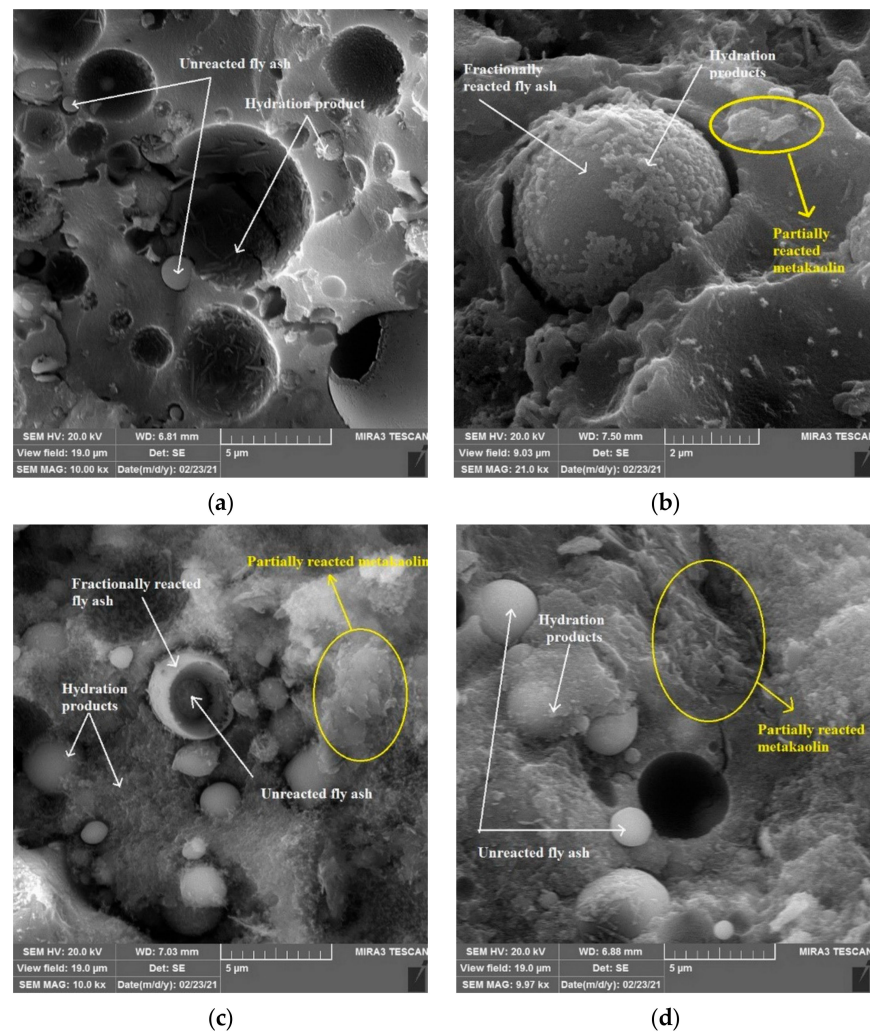


Figure 6. FESEM image of the geopolymer samples (a) GP₁₀₀₋₀; (b) GP₇₀₋₃₀, (c) GP₅₀₋₅₀; and (d) GP₃₀₋₇₀.

3.5. Compressive Strength

Compressive strength and specific density are shown in Figure 7. The factor that affects the most compressive strength is the alkalinity ratio. The deficit of solubilized Si and Al in the system leads to the formation of a geopolymer-matrix with some weak mechanical characteristics.

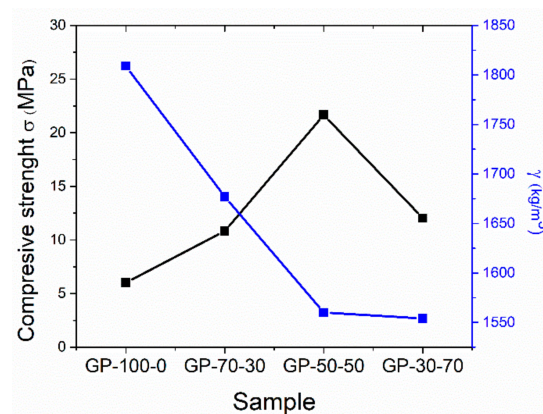


Figure 7. Compressive strength and specific density of geopolymer sample.

Otherwise, the deficit of alkaline ions could cause the participation of Al ions because it requires an alkaline ion for maintaining the charge equilibrium [32,33]. The presence of higher amounts of alkalis during geopolymerization led to the formation of products with high structural integrity. Literature data show that carbonate formation adversely affects the mechanical strength characteristics of geopolymers [34,35].

The $\text{SiO}_2/\text{Al}_2\text{O}_3$ molar ratio is one of the most influential parameters that affects the strength of geopolymer samples. The addition of silicon to the synthesis, through the activation solution, favors the synthesis of geopolymer products with improved mechanical performance. Additional silicon ions affect the formation of the geopolymer matrix by acting as nucleation sites for polycondensation reactions. Increasing the $\text{SiO}_2/\text{Al}_2\text{O}_3$ ratio through the activation solution ($\text{SiO}_2/\text{Al}_2\text{O}_3 > 3.00$) has a negative effect on the strength. Excess silicon ions in the activation solution limit the dissolution of aluminosilicate precursors.

The highest value of compressive strength is achieved in the case of the sample GP₅₀₋₅₀. Decreasing the compressive strength at the highest proportion of FA can be explained, as the pH value is high enough to dissolve the silicon from the raw material. At the same time, the strongest sample has also the lowest specific density. This indicates that the ratio of FA and MK 50:50 is optimal for this material. FA does affect favorably the compressive strength, but up to certain limits. The strength of the samples based on the FA/MK is not higher compared to the samples based on the metakaolin [36]. Due to the presence of some crystal phase, which to some extent strengthens the geopolymer matrix, but their content exceeds certain limits in the matrix, which leads to a violation of the homogeneity and the appearance of cracks through the matrix, and thus to a decrease in the compressive strength of the geopolymer concrete samples.

As can be observed from the graph, the compressive strength shows that fly ash-based geopolymer samples with a ratio of 0.5 had the highest strength which is 21.66 MPa. For the fly ash-based sample, the increase in the binder to MK ratio will lead the mixture to increase in compressive strength. However, it starts to decrease after a ratio of 0.5. This is due to there being insufficient binder to bind the aggregate for the ratio below 0.5 and the geopolymerization process provides insufficient gel to glue the MK particle. The addition of MK means the addition of a strong particle inside the sample [37]. Conclusively, the reduction of the MK percentage in the sample decreases the compressive strength of the fly ash-based geopolymer.

4. Conclusions

In order to obtain sustainable green materials, a low carbon-content geopolymer with good mechanical and chemical properties, four samples with different ratios of fly ash (FA) and metakaolin (MK) were prepared. The synthesis of geopolymers from two-component raw materials, metakaolin (MK) and fly ash (FA), confirmed that the best ratio is 50:50. The presence of kaolinite, quartz, wollastonite (calcium silicon oxide), and pyrophyllite (aluminum silicate) was confirmed using XRD analysis. The amorphous response in the range of $2\theta = 15\text{--}40^\circ$ does not show significant changes during the aging process of 28 days. DRIFT spectra of geopolymer samples based on fly ash and metakaolin as precursors confirmed the formation of a new aluminosilicate phase. Characteristic bands of the Si-O and O-Si-O groups were observed at 1045 cm^{-1} confirming the presence of silicate groups. XPS analysis shows that the total reaction rate of the sample with optimal stoichiometry is about 50%, with the almost complete absence of carbon. The process of coalescence and merging into larger spheres is noticeable on the SEM image of the sample with the highest compressive strength. The compressive strength of the FA/MK-based geopolymer samples shows an increasing trend up to a FA/MK ratio of 50:50 where it takes the highest value of 21.7 MPa. Based on the results obtained in this study, it can be concluded that fly ash-based geopolymer, can be a good replacement for Portland cement in the building industry as a low cost and eco-friendly construction material. This research also indicates the potential use of the alkali-activated materials for different purposes (such as geopolymer systems

which overcome the shortcoming regarding fragility), which can be a great stimulus to adjust or develop the up-scaled technology.

Author Contributions: S.N. conceived and designed the experiments, wrote the paper, and contributed to all the experiments and analyzing of the obtained results; M.N. gave his contribution due to conceptualization (ideas; formulation or evolution of research goals and aims) and contributed in detailed XPS acquiring and analysis; J.G. conducted the SEM analysis and contributed to the writing of the paper; L.K. completed the supervision and leadership responsibility for the research activity planning and implementation, including mentorship to the research team; M.M. contributed in analyzing the XRD results; M.V. and I.B. performed the mechanical characterization. All authors have read and agreed to the published version of the manuscript.

Funding: The research was funded by the Ministry of Education, Science and Technological Development of the Republic of Serbia—(Vinca Institute of Nuclear Sciences—grant No. 1702202, grant No. 1702205 and grant No. 0402205). The work is also the result of a bilateral project between Serbia and Montenegro No. 451-03-02263/2018-09/20.

Institutional Review Board Statement: Not applicable.

Informed Consent Statement: Not applicable.

Data Availability Statement: Not applicable.

Conflicts of Interest: The authors declare no conflict of interest.

References

1. Nenadović, S.; Mucsi, G.; Kljajević, L.J.; Mirković, M.; Nenadović, M.; Kristaly, F.; Vukanac, I. Physicochemical, mineralogical and radiological properties of red mud samples as secondary raw materials. *Nucl. Technol. Radiat. Prot.* **2017**, *32*, 261–266. [[CrossRef](#)]
2. Bosković, I.; Nenadović, S.; Kljajević, L.J.; Vukanac, I.; Stankovic, N.; Luković, J.; Vukčević, M. Radiological and Physicochemical Properties of Red Mud Based Geopolymers. *Nucl. Technol. Radiat. Prot.* **2018**, *33*, 188–194. [[CrossRef](#)]
3. Bosković, I.; Vukčević, M.; Nenadović, S.; Mirković, M.; Stojmenović, M.; Pavlović, V.; Kljajević, L.J. Characterization of red mud/metakaolin-based geopolymers as modified by Ca(OH)₂. *Mater. Tehnol.* **2019**, *53*, 341–348. [[CrossRef](#)]
4. Kljajević, L.J.; Nenadović, S.; Nenadović, M.; Bundaleski, N.; Todorović, B.; Pavlović, V.; Rakočević, Z. Structural and Chemical Properties of Thermally Treated Geopolymer Samples. *Ceram. Inter.* **2017**, *43*, 6700–6708. [[CrossRef](#)]
5. Nenadović, S.; Claudio, F.; Nenadovic, M.; Raffaele, C.; Mirković, M.; Vukanac, I.; Kljajevic, L.J. Chemical, physical and radiological evaluation of raw materials and geopolymer for building application. *J. Radioanal. Nucl. Chem.* **2020**, *325*, 435–445. [[CrossRef](#)]
6. Ivanović, M.; Kljajević, L.J.; Gulicovski, J.; Petković, M.; Janković-Častvan, I.; Bučevac, D.; Nenadović, S. The effect of the concentration of alkaline activator and aging time on the structure of metakaolin based geopolymer. *Sci. Sinter.* **2020**, *52*, 219–229. [[CrossRef](#)]
7. Nenadović, S.; Kljajević, L.J.; Nešić, M.; Petković, M.; Trivunac, K.; Pavlović, V. Structure analysis of geopolymers synthesized from clay originated from Serbia. *Environ. Earth Sci.* **2017**, *13*, 76–79. [[CrossRef](#)]
8. Mladenović, N.; Kljajević, L.J.; Nenadović, S.; Ivanović, M.; Čilija, B.; Gulicovski, J.; Trivunac, K. The Applications of New Inorganic Polymer for Adsorption Cadmium from WasteWater. *Inorg. Organomet. Polym. Mater.* **2020**, *30*, 554–563. [[CrossRef](#)]
9. Ivanović, M.; Kljajević, L.J.; Nenadović, M.; Bundaleski, N.; Vukanac, I.; Todorović, B.; Nenadović, S. Physicochemical and radiological characterization of kaolin and its polymerization products. *Constr. Build. Mater.* **2018**, *68*, 330.e155. [[CrossRef](#)]
10. Naidu, G.; Prasad, A.S.S.N.; Adishesu, S.; Satayanarayana, P.V.V. A Study on Strength Properties of Geopolymer Concrete with addition of GGBS. *Int. J. Eng. Res.* **2012**, *2*, 19–28.
11. Zhuang, X.Y.; Chen, L.; Komarneni, S.; Zhou, C.H.; Tong, D.S.; Yang, H.M.; Yu, W.H.; Wang, H. Fly Ash-based Geopolymer: Clean Production, Properties and Applications. *J. Clean. Prod.* **2016**, *125*, 253–267. [[CrossRef](#)]
12. Kljajević, L.J.; Melichova, Z.; Kisić, D.; Nenadović, M.; Todorović, B.; Pavlović, V.; Nenadović, S. The influence of alumino-silicate matrix composition on surface hydrophobic properties. *Sci. Sint.* **2018**, *51*, 163–173. [[CrossRef](#)]
13. Kljajević, L.J.; Melichova, Z.; Stojmenović, M.; Todorović, V.; Čitaković, N.; Nenadović, S. Structural and electrical properties of geopolymer materials based on different precursors (kaolin, bentonite and diatomite). *Maced. J. Chem. Chem. Eng.* **2019**, *38*, 283–292. [[CrossRef](#)]
14. Kioupis, D.; Kavakakis, C.; Tsivilis, S.; Kakali, G. Synthesis and Characterization of Porous Fly Ash-Based Geopolymers Using Si as Foaming Agent. *Adv. Mater. Sci. Eng.* **2018**, *2018*, 1942898. [[CrossRef](#)]
15. Samson, G.; Cyr, M.; Gao, X.X. Formulation and characterization of blended alkali-activated materials based on flash-calcined metakaolin, fly ash and GGBS. *Constr. Build. Mater.* **2017**, *144*, 50–64. [[CrossRef](#)]
16. Petrillo, A.; Cioffi, R.; Ferone, C.; Colangelo, F.; Borerilli, C. Eco-sustainable geopolymer concrete blocks production process. *Agric. Sci. Procedia* **2016**, *8*, 408–418. [[CrossRef](#)]

17. Pacheco-Torgal, F.; Abdollahnejad, Z.; Miraldo, S.; Baklouti, S.; Ding, Y. An overview on the potential of geopolymers for concrete infrastructure rehabilitation. *Constr. Build. Mater.* **2012**, *36*, 1053–1058. [[CrossRef](#)]
18. Emmons, P.H. The Concrete Repair Industry, Actions for Improvements. In *Concrete Repair, Rehabilitation and Retrofitting III*, 1st ed.; Taylor & Francis group: London, UK, 2012; pp. 13–14.
19. Nenadović, S.; Kljajević, L.J.; Nenadović, M.; Mirković, M.; Marković, S.; Rakočević, Z. Mechanochemical treatment and structural properties of lead adsorption on kaolinite (Rudovci, Serbia). *Environ. Earth Sci.* **2015**, *73*, 7669–7677. [[CrossRef](#)]
20. Mackenzie, K.; Brown, I.; Meinhold, R.H.; Bowden, M.E. Thermal Reactions of Pyrophyllite Studied by High-Resolution Solid-state ²⁷Al and ²⁹Si Nuclear Magnetic Resonance Spectroscopy. *J. Am. Ceram. Soc.* **2006**, *68*, 266–272. [[CrossRef](#)]
21. Provis, J.L.; Van Deventer, J.S.J. *Geopolymers, Structures, Processing, Properties and Industrial Applications*; Woodhead Publishing: Abingdon, UK, 2009; pp. 294–312.
22. Ouahabi, M.; Daoudi, L.; Hatert, F.; Fagel, N. Modified Mineral Phases During Clay Ceramic Firing. *Clays Clay Min.* **2015**, *63*, 404–413. [[CrossRef](#)]
23. Ibarra, J.; Moliner, R.; Bonet, A.J. FT-i.r. investigation on char formation during the early stages of coal pyrolysis. *Fuel* **1994**, *73*, 918–924. [[CrossRef](#)]
24. Kaya, K.; Soyer-Uzun, S. Evolution of structural characteristics and compressive strength in red mud–metakaolin based geopolymer systems. *Ceram. Int.* **2016**, *42*, 7406–7413. [[CrossRef](#)]
25. van de Marel, H.W. *Beutespacher Atlas of Infrared Spectroscopy of Clay Minerals and Their Mixtures*; Elsevier: New York, NY, USA, 1976; pp. 1–319.
26. Ferone, C.; Colangelo, F.; Cioffi, R.; Montagnaro, F.; Santoro, L. Use of reservoir clay sediments as raw materials for geopolymer binders. *Adv. Appl. Ceram.* **2013**, *112*, 184–189. [[CrossRef](#)]
27. Ferone, C.; Liguori, B.; Capasso, I.; Colangelo, F.; Cioffi, R.; Cappelletto, E.; Di Maggio, R. Thermally treated clay sediments as geopolymer source material. *Appl. Clay Sci.* **2015**, *107*, 195–204. [[CrossRef](#)]
28. Provis, J.; Rees, C. *Geopolymer Synthesis Kinetics, Geopolymers: Structures, Processing, Properties and Industrial Applications*; Woodhead Publishing: Abingdon, UK, 2009; pp. 118–136.
29. Innocenzi, P. Infrared spectroscopy of sol-gel derived silica-based films: A spectra-microstructure overview. *J. Non. Cryst. Solids* **2003**, *316*, 309–319. [[CrossRef](#)]
30. Yin, Y.; Yin, H.; Wu, Z.; Qi, C.; Tian, H.; Zhang, W. Characterization of Coals and Coal Ashes with High Si Content Using Combined Second-Derivative Infrared Spectroscopy and Raman Spectroscopy. *Crystals* **2019**, *9*, 513. [[CrossRef](#)]
31. Samson, G.; Cyr, M.; Xiao, G. Termomechanical performance of blended metakaolin-GGBS alkali-activated foam concrete. *Constr. Build. Mater.* **2017**, *157*, 982–993. [[CrossRef](#)]
32. Duxson, P.; Mallicoat, S.W.; Lukey, G.C.; Kriven, W.M.; Van Deventer, J.S.J. The effect of alkali and Si/Al ratio on the development of mechanical properties of metakaolin-based geopolymers. *Coll. Surf. A Physicochem. Eng. Asp.* **2007**, *292*, 8–20. [[CrossRef](#)]
33. Xu, H.; Van Deventer, J.S.J. The Geopolymerisation of Alumino-Silicate Minerals. *Int. J. Miner. Process.* **2000**, *59*, 247–266. [[CrossRef](#)]
34. Kioupis, D.; Skaropoulou, A.; Tsvivilis, S.; Kakali, G. Valorization of Brick and Glass CDWs for the Development of Geopolymers Containing More Than 80% of Wastes. *Minerals* **2020**, *10*, 672. [[CrossRef](#)]
35. Criado, M.; Palomo, A.; Fernandez-Jimenez, A. Alkali activation of fly ashes. Part 1: Effect of curing conditions on the carbonation of the reaction products. *Fuel* **2005**, *84*, 2048–2054. [[CrossRef](#)]
36. Kljajević, L.J.; Nenadović, S.; Mirković, M.; Stojmenović, M.; Egelja, A.; Trivunac, K.; Stevanović, S. Characterization of Metakaolin Based Geopolymers. In Proceedings of the 3th Conference of the Serbian Society for the Ceramic Materials, Programme and Book of Abstracts, Belgrade, Serbia, 15–17 June 2015; Institute for Multidisciplinary Research, University of Belgrade: Belgrade, Serbia, 2015; p. 97.
37. Tayeh, B.A.; Abu Bakar, B.H.; Megat Johari, M.A.; Voo, Y.L. Evaluation of Bond Strength between Normal Concrete Substrate and Ultra High Performance Fiber Concrete as a Repair Material. *Procedia Eng.* **2013**, *54*, 554–563. [[CrossRef](#)]